

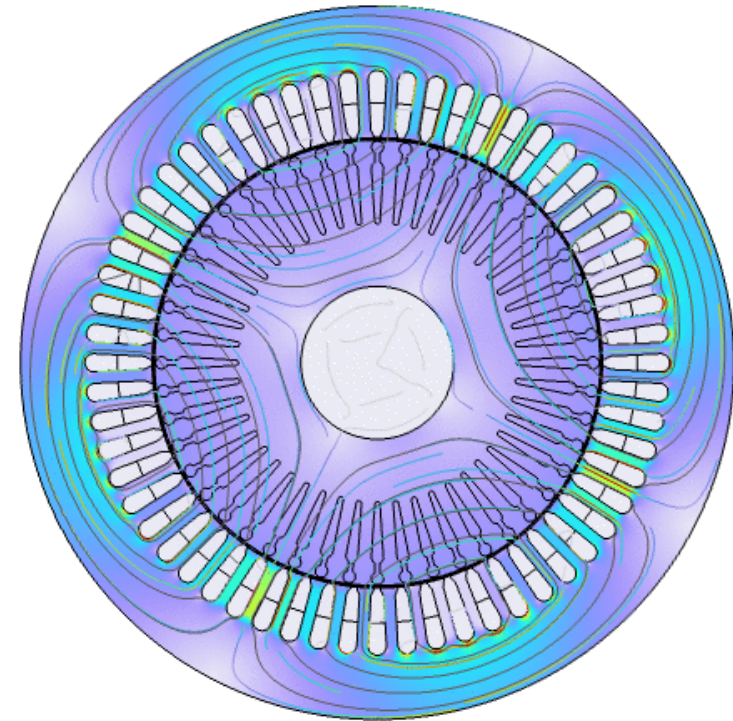
COMSOL Conference, Bengaluru, India

Modeling of the Static Eccentricity Type of Fault in Squirrel Cage Induction Motor by Using COMSOL 6.0

Rakesh Deore¹, Gopinath Sengupta², Bipul Brahma¹, Shahrukh¹,
Karuna Kalita¹

1. Department of Mechanical Engineering, IIT Guwahati,
Guwahati, Assam, India.

2. School of Energy Science and Technology, IIT Guwahati,
Guwahati, Assam, India.



30 Nov to 1 Dec, 2023

Content

- Introduction
- Faults and Causes
- Unbalanced Magnetic Pull (UMP)
- Numerical Modelling of UMP
- Result and Discussion
- Conclusion
- References



Introduction

- Electric machines are rotordynamic machines which converts electrical energy to mechanical energy or vice versa.
- **Induction Machines**

Widely used in domestic, commercial as well as industrial purpose (90%)

Robustness, Self starting, Economical, Reliable, Low maintenance

Types

Wound Rotor or Slip-ring Rotor

Squirrel Cage Rotor

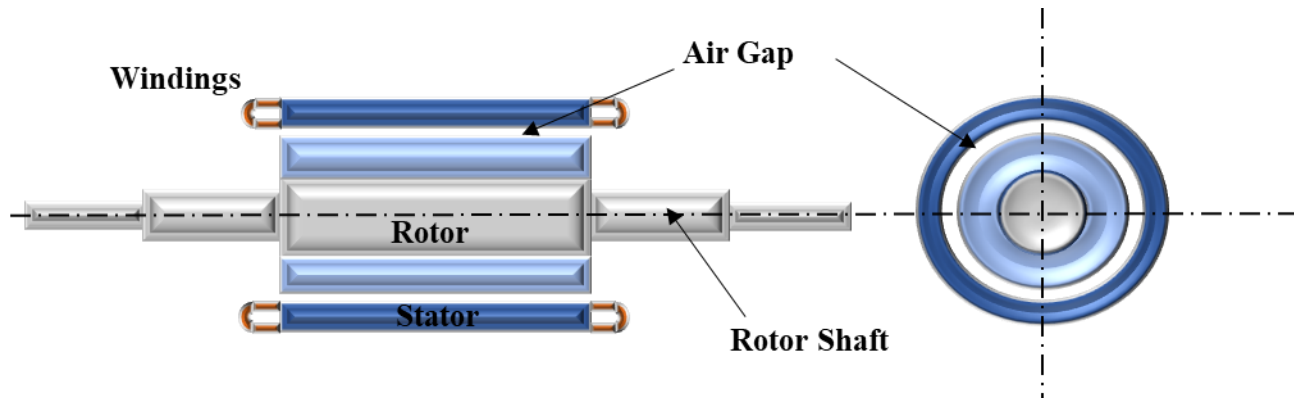
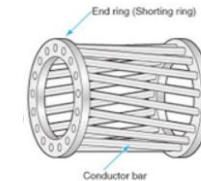
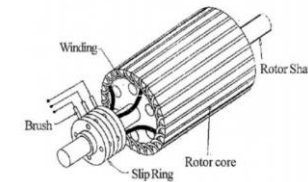


Fig. 1 Cross Section of an Induction Motor

The stationary part fixed hollow annular part is called as **stator**.

The rotating part or core is called as **rotor**.

Faults and Causes

- The fault occurrence possibility of different types of faults in induction motors is presented by the **Salah et al. [1]**.
- This fault may leads to the catastrophic failure so to avoid that they also discussed the detection methods for the faults.
- Faults arise due to the air gap between the stator and rotor is main concern.

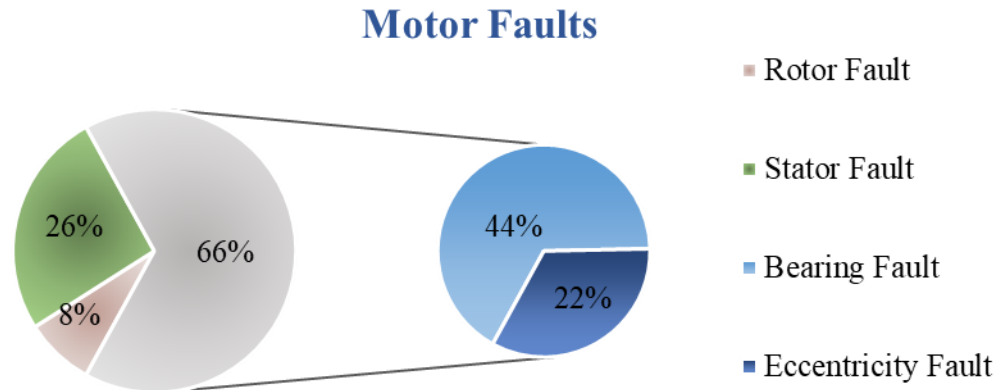


Fig. 2 Statistics of Faults in the Induction Motors

Eccentricity: Offset between rotor and stator

- Manufacturing tolerances,
- Assembly inaccuracy or miss alignment of the parts,
- Bend in rotor shaft,
- Wear and tear of bearings,
- Rotor and stator mechanical or electrical faults or a combination of both,
- Mass unbalance,
- Rotor operation at critical speed, etc.

Unbalanced Magnetic Pull (UMP)

- Ideally, the magnetic flux density distribution over the air gap is symmetric.
- But if there is any eccentricity, the rotor eccentricity creates asymmetry in the magnetic flux density distribution over the air gap by introducing the additional magnetic fields [2, 3].
- It produces the concentrated magnetic flux density due to which there will be the magneto motive force (MMF) is generated in the area of the smallest air gap.

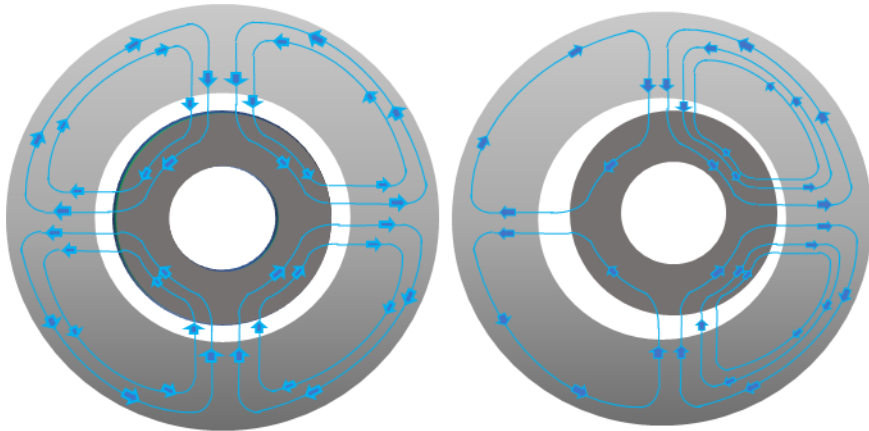


Fig 3: Flux Distribution of an Ideal Rotor and an Eccentric Rotor

Effects of UMP

The net electromagnetic force toward the smallest air gap leads to,

- Rubbing of the rotor and stator.
- Wear and tear of the bearing.
- Further increase of the eccentricity.
- May be catastrophic failure of the rotor bar.
- Increase vibration and noise.

A 2D numerical electromagnetic analysis on a bridge configured induction motor for Bridge OFF condition using the COMSOL Multiphysics software version 6.0 which is based on FEM

- Electric flux density is not conservative, and given by the Gauss's law as; $\nabla \cdot \vec{E} = \rho$
- Time derivative of magnetic flux density can generate electric field, given by Faraday's Law as; $\nabla \times \vec{E} = -\frac{\partial \vec{B}}{\partial t}$
- Magnetic field is conservative and given as; $\nabla \cdot \vec{B} = 0$
- Magnetic field can create split into conduction current and time derivative of electrical flux density, and given by Ampere's law as; $\nabla \times \vec{H} = \vec{J} + \frac{\partial \vec{D}}{\partial t}$

The constitutive equations are as follows,

- Ohm's law in point or local form is given as; $\vec{J} = \sigma \vec{E}$

H	Magnetic field intensity
J	Current density
D	Electric flux density
B	Magnetic flux density
E	Electric flux intensity
ρ	Charge density
σ	Electric conductivity

Numerical Modelling UMP

The magnetic vector potential in Eq. $\nabla \times \vec{H} = \vec{J} + \frac{\partial \vec{D}}{\partial t}$ is solved in every node in a two-dimensional problem formulation. Where, the magnetic flux density is the curl of the magnetic vector potential, i.e. $\vec{B} = \nabla \times \vec{A}$

The equation is solved for the out of the plane magnetic vector component only which implies that the in-plane currents and out of the plane magnetic fields are neglected. This is just the assumption for the 2D problem

For convenience the machine in three sub-domains: Stator, Rotor and Airgap

$$\nabla \times \left(\frac{1}{\mu_0 \mu_r} \nabla \times A \right) = J^e \quad \Rightarrow \quad \text{Winding conductors (eddy-current effects neglected.)}$$

$$\nabla \times \left(\frac{1}{\mu_0 \mu_r} \nabla \times A \right) = 0 \quad \Rightarrow \quad \text{Iron core Rotor and Stator both}$$

$$\nabla \times \left(\frac{1}{\mu_0} \nabla \times A \right) = 0 \quad \Rightarrow \quad \text{Airgap}$$

Steps in Modelling

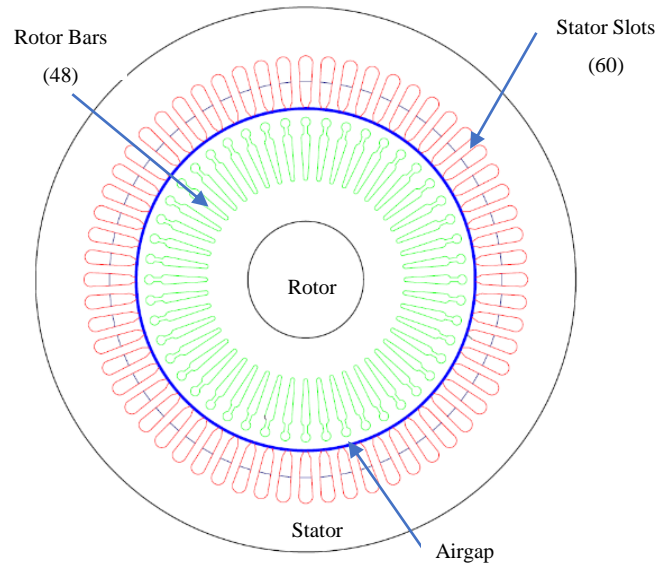


Fig.44 2D Cross Section of Rotor Stator Assembly.

Sr. No	Parameters	Values
1	Stator outer diameter (mm)	350
2	Stator inner diameter (mm)	221
3	Coil diameter (mm)	1.22
4	Rotor outer diameter (mm)	218.5
5	Airgap (mm)	1.25
6	Length of the Stator/rotor core	0.21
7	No of Turns	11
8	No. of strands	3

Table 2 Parameters of the Machine.

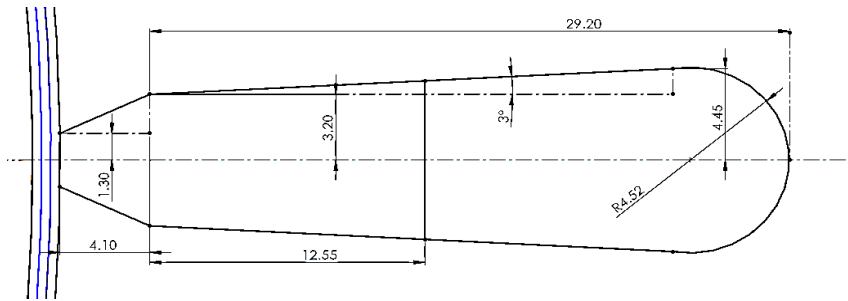


Fig.5 Dimensions of Stator Slots.

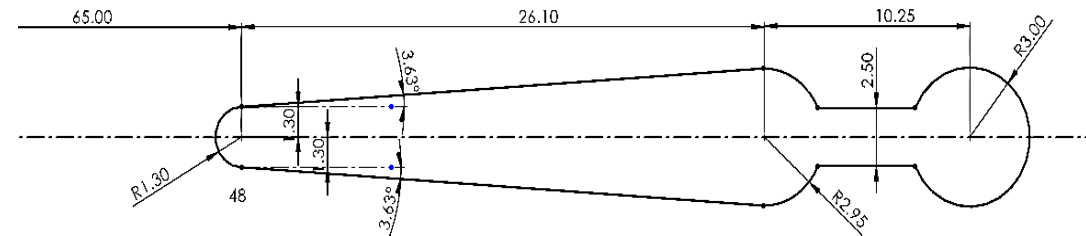


Fig.6 Dimensions of Rotor Bar.

Steps in Modelling

- Ultimately, we can find the flux distribution & UMP in the airgap so the modeling of the airgap is an important thing.
- Thus, the airgap is divided into three parts one part is modeled with a rotor and 2 parts with a stator.

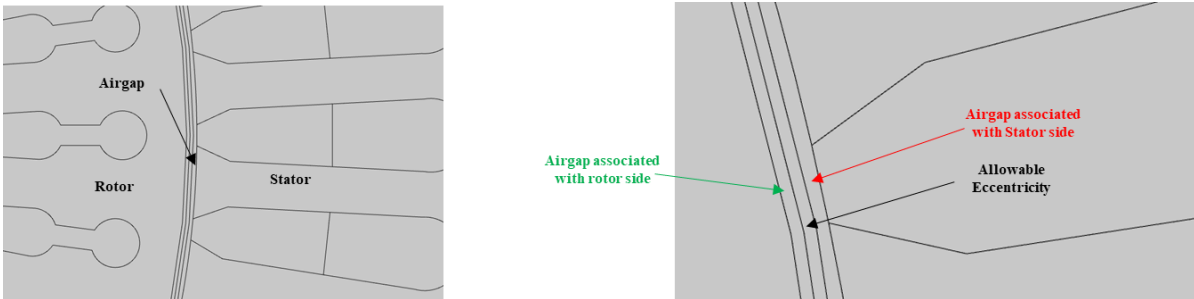


Fig.7 Modelling of airgap

Default the physics-controlled mesh is generated, which has the free three noded elements.

And Moving Mesh is implemented to the rotor and rotor side airgap

Sr. No	Parts	Material Assigned
1	Stator Core	Soft Iron
2	Rotor Core	Soft Iron
3	Air Gap	Air
4	Coils	Copper
5	Rotor bars	Aluminium
6	Shaft	SS303

Table 3 Material Used in Components.

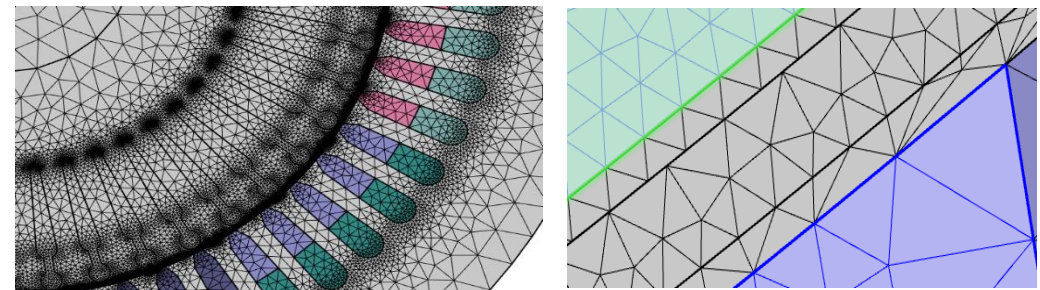
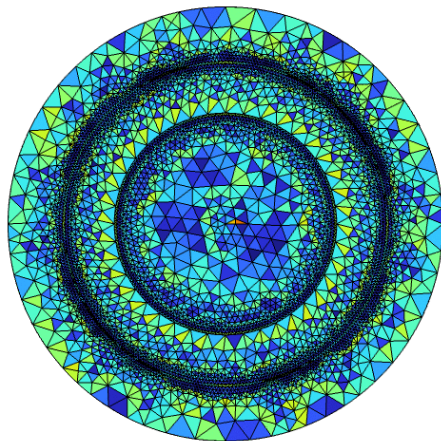


Fig.8 Meshed Model

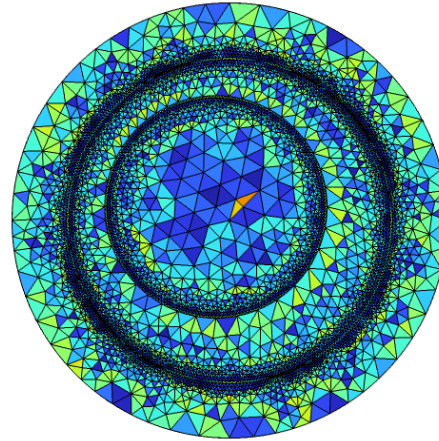
Type of Eccentricities Modelled

By explained steps, the 2D electromagnetic behavior of the induction motor is modeled for the 5A sinusoidal current input to each phase at a phase difference of the 120^0 without circuit equation bridge-OFF condition.

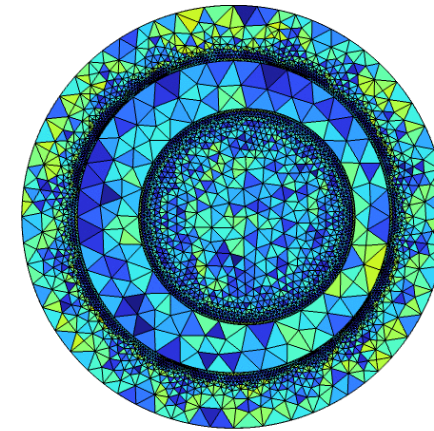
First, the concentric rotor-stator assembly is simulated. And later the effect of the eccentricity between the rotor and stator is modeled for the Static eccentricity case. And the effect of variable % of eccentricity is also explained.



Concentric



Static Eccentricity



Dynamic Eccentricity

Fig 9: Modelled Eccentricities

Result & Discussion

The simulation for the induction motor running at 1470 rpm is run for 0.1 sec. and the results are produced for the concentric rotor and the rotor with 10% eccentricity in x direction only.

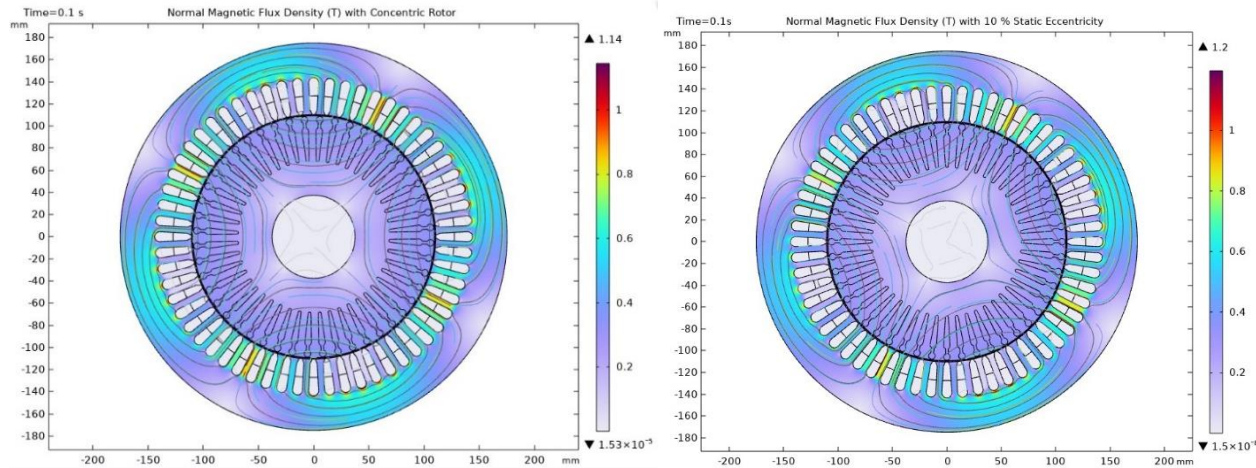


Fig. 10 a) Magnetic Flux Density with Concentric Rotor b) Magnetic Flux Density with 10 % Static Eccentric Rotor

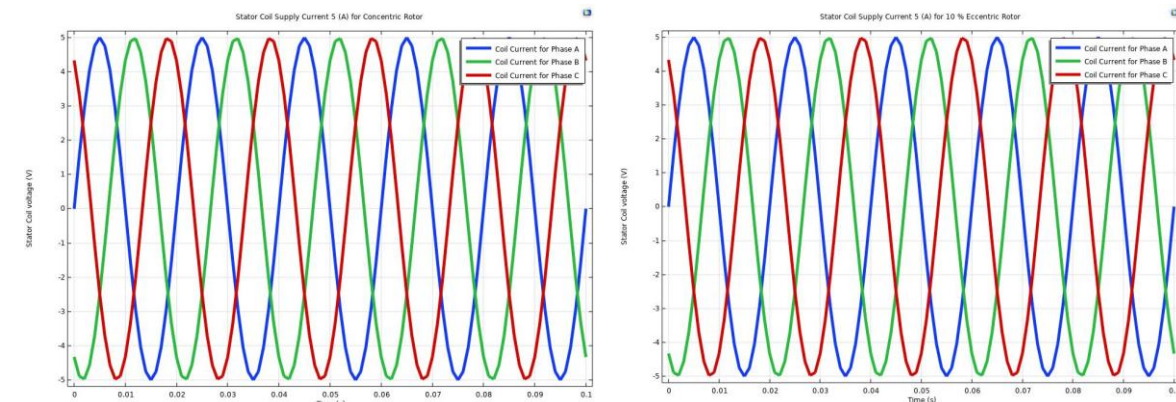


Fig. 11 a) Current Profile in Coils with Concentric Rotor b) Current Profile in Coils with 10% Static Eccentric Rotor

It is found that in case of the concentric rotor and the 10 % eccentric rotor the maximum flux density in the eccentric rotor cross section is 5.263 % greater than the concentric cross section.

Result & Discussion

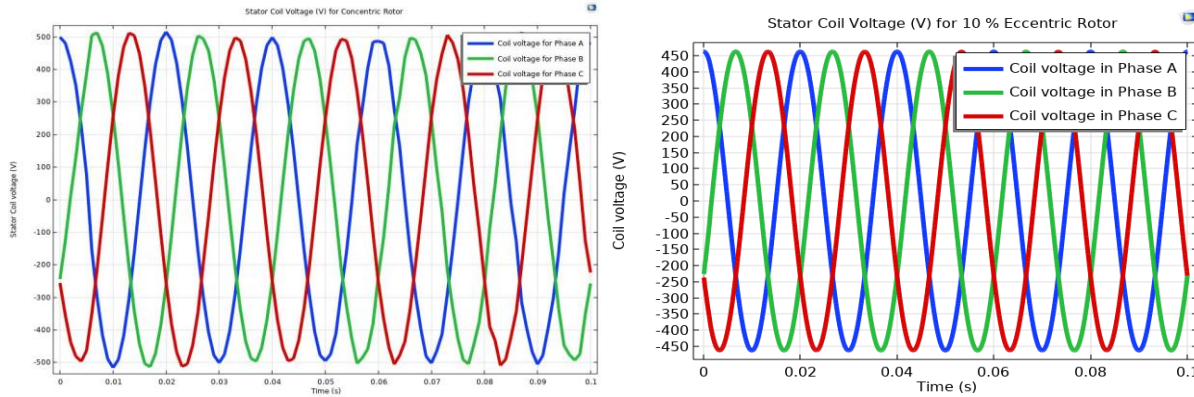
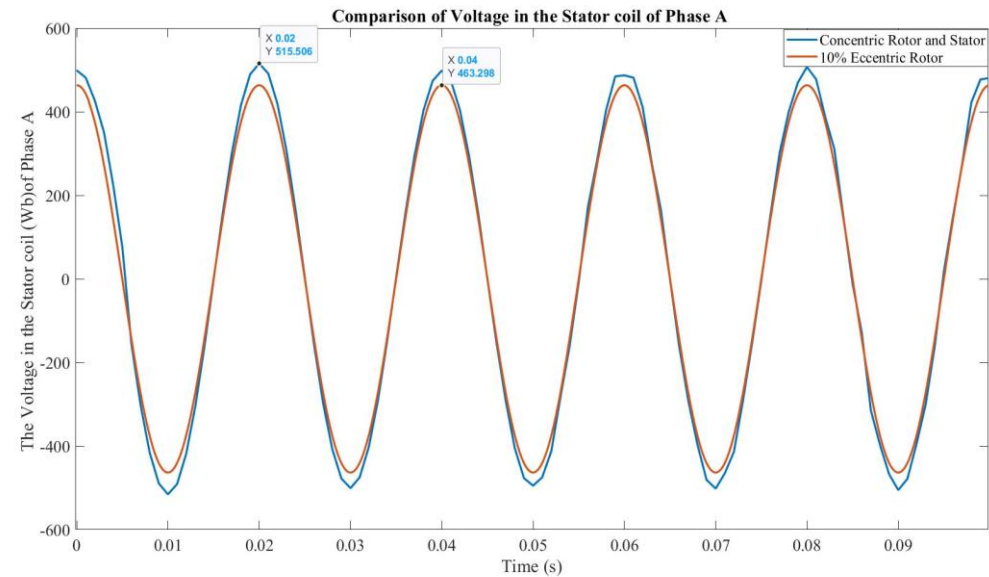


Fig. 12 a) Voltage Profile in Coils with Concentric Rotor b) Voltage Profile in Coils with 10% Static Eccentric Rotor



It has been seen that the stator coil voltage for the concentric rotor is around 515V, & for the 10 % eccentric rotor stator coil voltage produced due to 5A current supply to the star connected induction motor is around 463V.

The voltage produced in the 10 % eccentric rotor stator coil is 10.1 % lesser than the voltage produced in the 0 % eccentric rotor configuration.

Result & Discussion

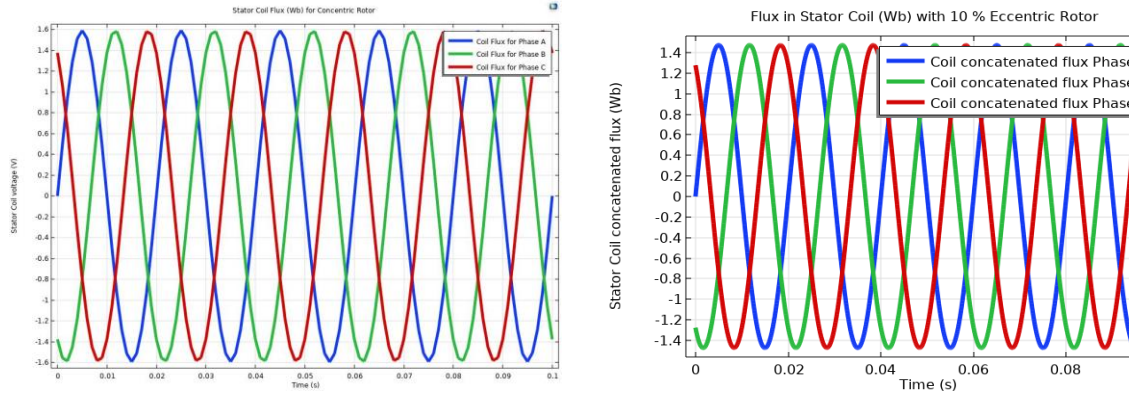
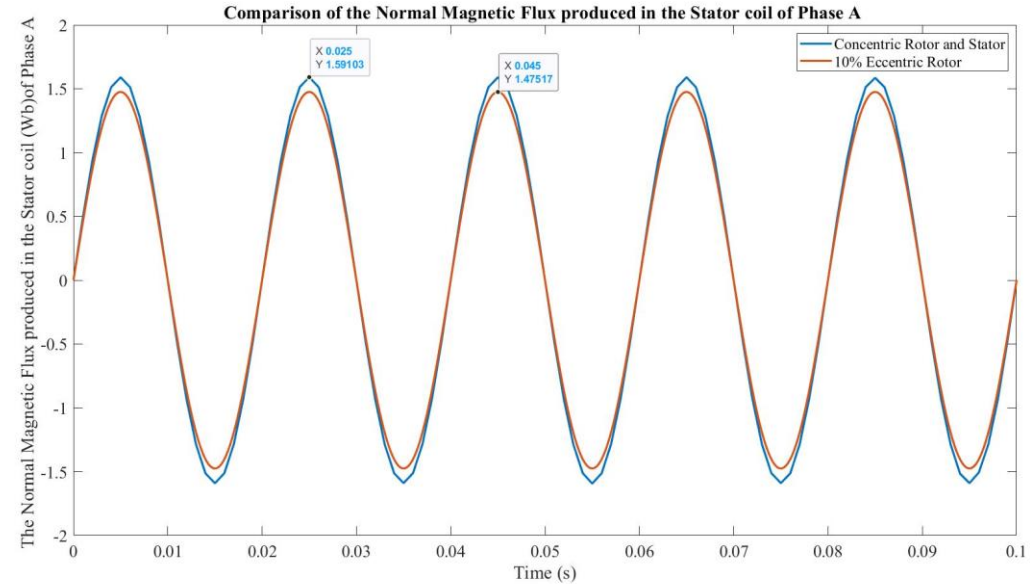


Fig.13 a) Flux (Wb) Profile in Stator Coils with Concentric Rotor b) Flux (Wb) Profile in Stator Coils with 10% Static Eccentric Rotor.



It has been noticed that the flux produced in each stator coil per phase is get reduced from 1.5901Wb to 1.47517Wb in case of 10 % eccentric rotor compared to concentric configuration.

The normal flux produced in the stator coils of the concentric rotor is 7.24 % greater than the normal flux produced in the stator coils of the 10 % eccentric rotor.

Result & Discussion

Variation of the Radial Magnetic Flux Density of the Airgap at a distance of the 109.5 mm from rotor Center w.r.t Arc Length of the Airgap

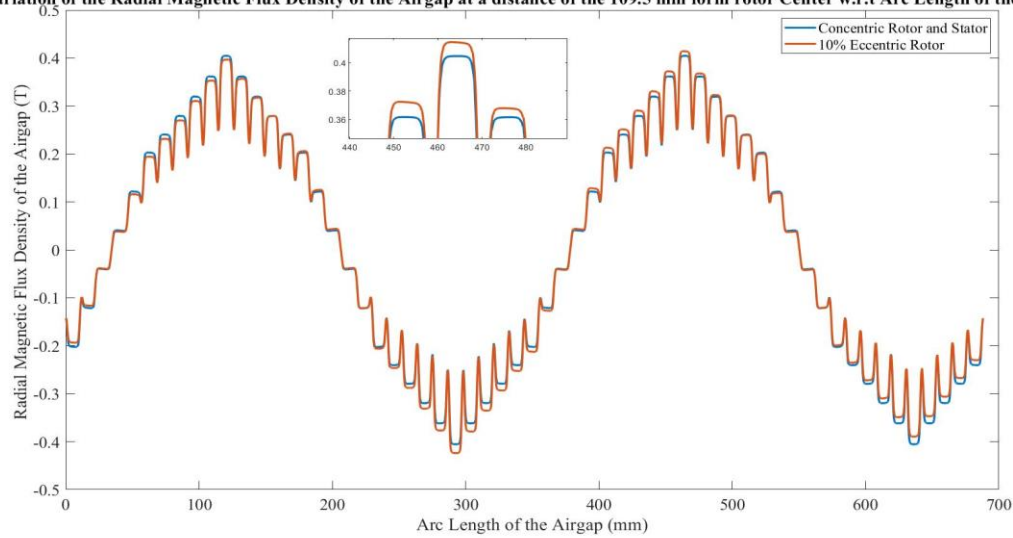


Fig. 14 Comparison of Airgap flux density in Concentric Rotor & 10% Static Eccentric Rotor w.r.t Arc Length of the Airgap Layer at 109.5 mm

Variation of the Radial Magnetic Flux Density of the Airgap w.r.t Angular Position

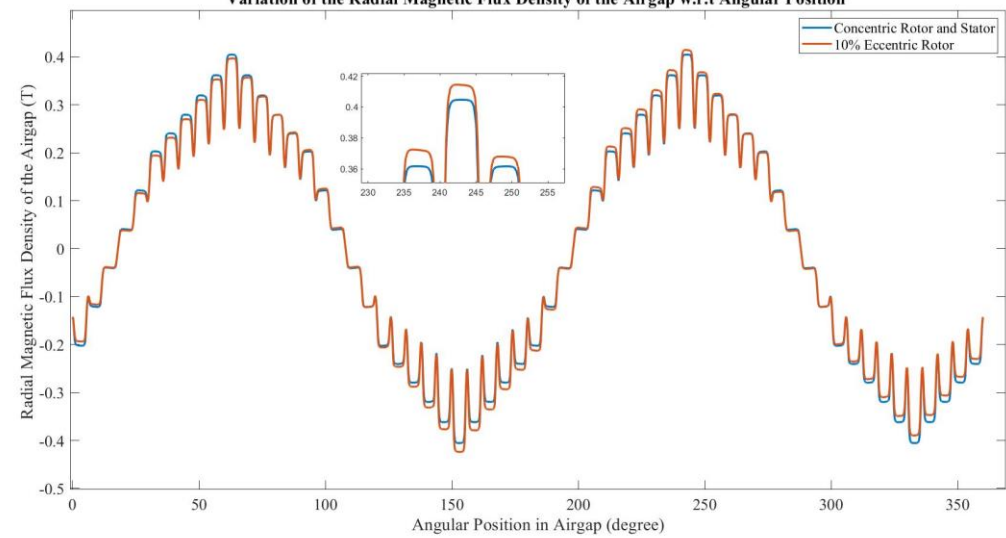
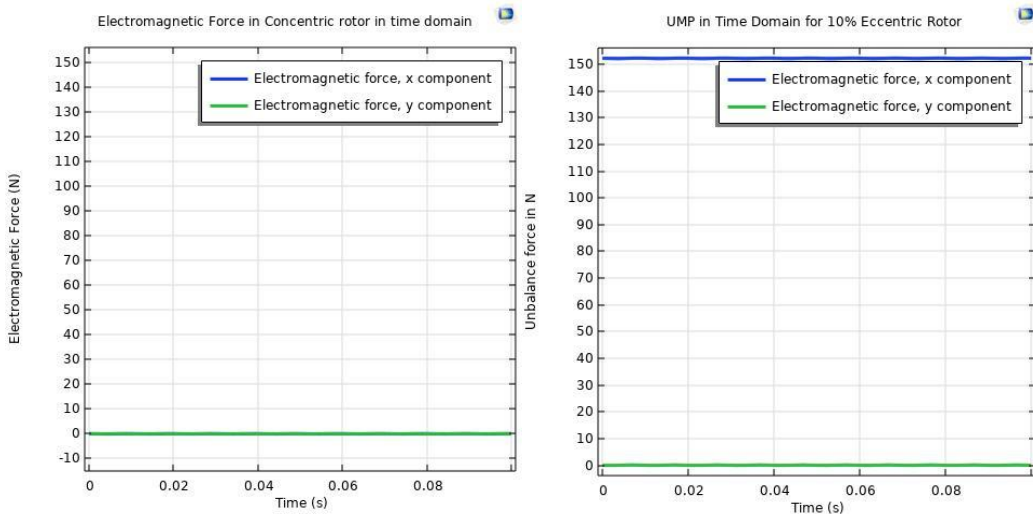


Fig. 15 Comparison of Airgap flux density in Concentric Rotor & 10% Static Eccentric Rotor w.r.t Angular Position of the Airgap Layer at 109.5 mm

The air gap flux density in the airgap layer is uniform in case of the concentric rotor-stator assembly, but due to eccentricity the air gap flux density is non-uniform in case of the eccentric rotor.

The maximum magnitude of the normal airgap flux density for Concentric rotor is 0.4T , Whereas, for 10 % eccentric rotor the magnitude of the airgap flux density at a point in direction of minimum airgap is 0.423T and at maximum airgap is 0.389T

Result & Discussion



The maximum magnitude of the unbalanced force is 152.0 N

Inherently in case of the parallel winding there is force component at $2f_s$ (here 100 Hz) and due to the static eccentricity, there are two force components at 0 Hz and at $2f_s$ (here 100 Hz).

[6]

Fig. 16 Comparison of UMP in time domain a) Concentric Rotor b) 10% Static Eccentric Rotor.

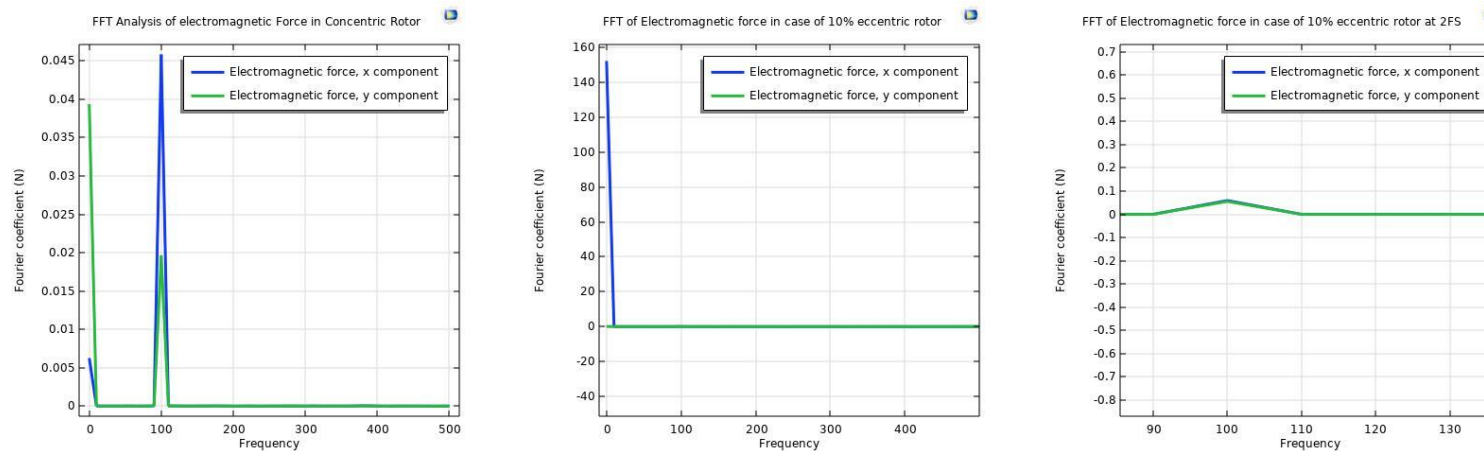


Fig. 17 Comparison of FFT of UMP component in a) Concentric Rotor b) 10% Static Eccentric Rotor at 0Hz c) 10% Static Eccentric Rotor at 100Hz

Result & Discussion

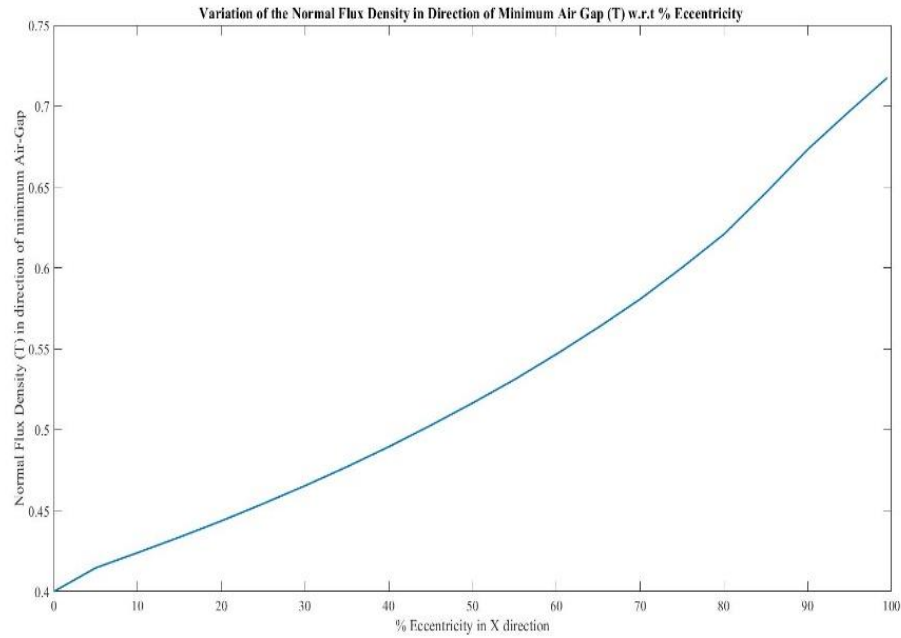


Fig. 18 Variation of Airgap Flux Density w.r.t % Eccentricity in Direction of the Minimum airgap

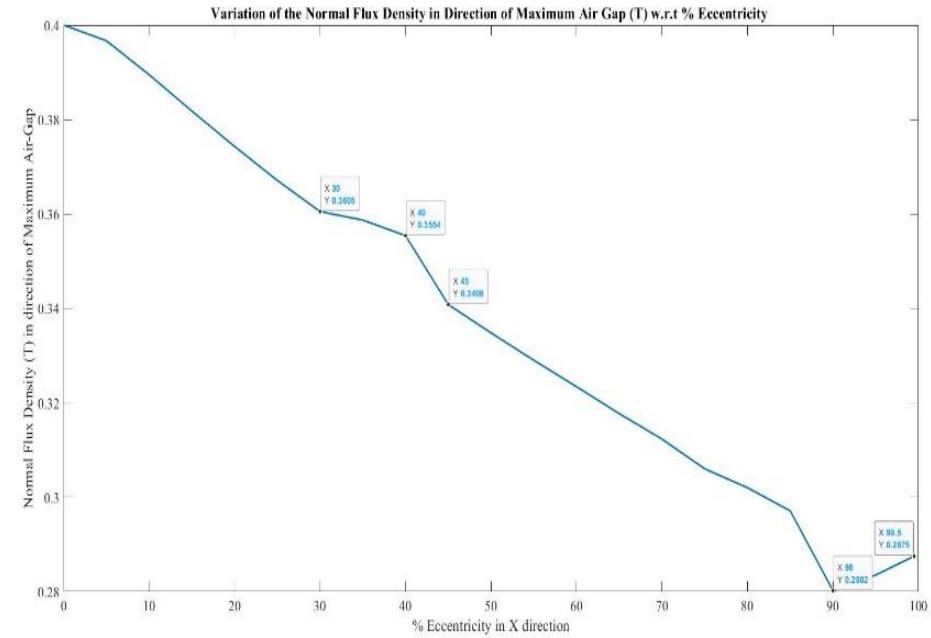


Fig. 19 Variation of Airgap Flux Density w.r.t % Eccentricity in Direction of the Maximum Airgap

For minimum airgap the magnetic flux density is increased from 0.414 T to 0.7173 T for the % eccentricity increased from 5 % to 99.5 %

For Maximum airgap the magnetic flux density is decreased from 0.3967 T to 0.2875 T for the % eccentricity increased from 5 % to 99.5 %

Result & Discussion

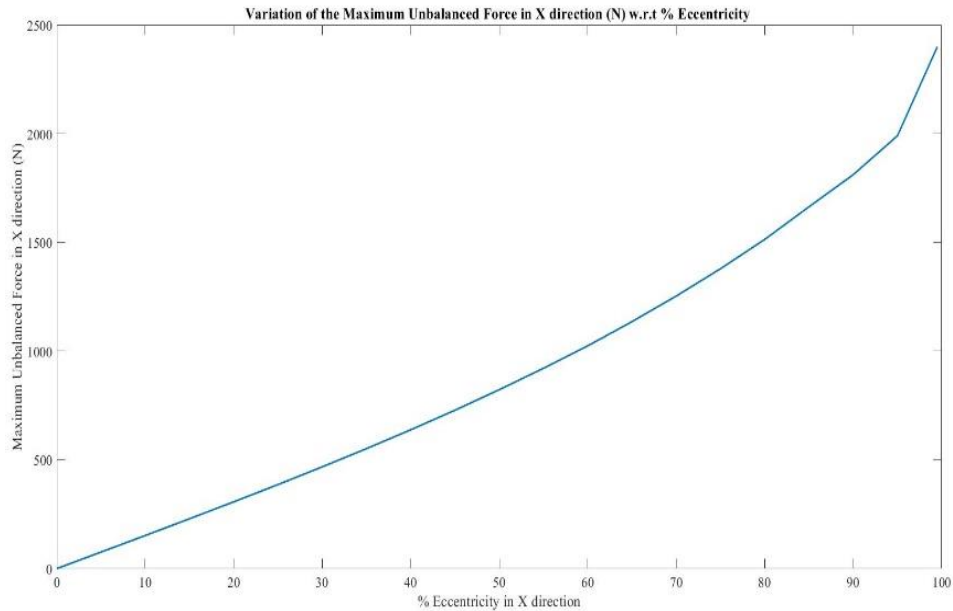


Fig. 20 Variation of UMP w.r.t % Eccentricity at 0 Hz

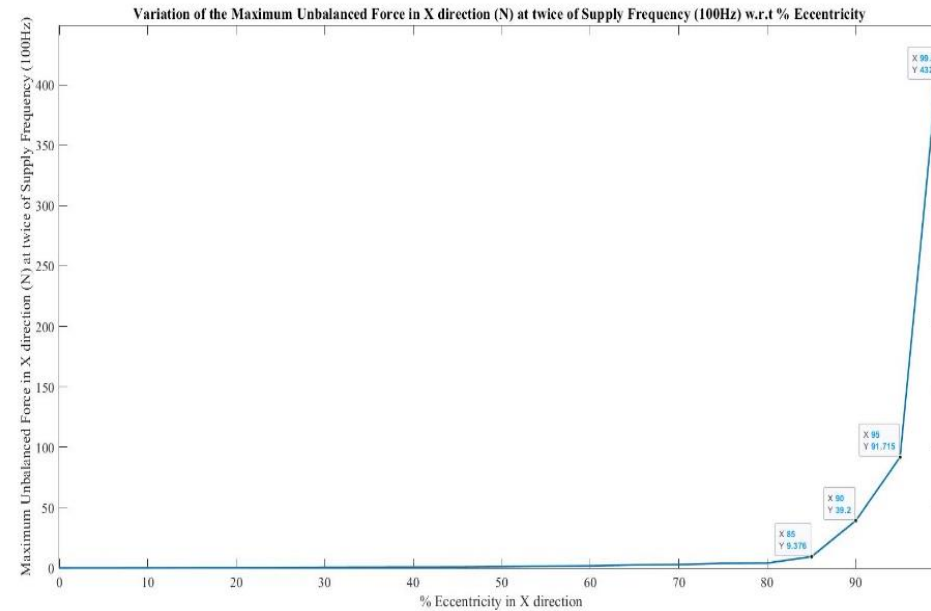


Fig. 21 Variation of UMP w.r.t % Eccentricity at 100 Hz

In case of the concentric configuration this unbalanced force was 0 N and with the increase of the eccentricity from 5% to the 99.5%, the unbalanced force is also increased from 76 N to 2400 N at 0 Hz and for 100 Hz it is increased from 0.048 N to 432N.

From Numerical Modelling

- ❑ No unbalanced force in case of the concentric rotor but case of the 10% eccentric rotor there is force component at 0 Hz and 100 Hz frequency.
- ❑ Static eccentricity causes the UMP at 0 Hz and $2f_s$ frequency which are dominant in nature and same conclusion is found from the analytical analysis of the UMP for a case of the static eccentricity.
- ❑ As the eccentricity increases, the airgap flux in direction of the minimum airgap is also increases and in the direction of the maximum air gap decreases.
- ❑ As the eccentricity increases the constant component of the UMP at 0 Hz also increases and another component at twice the supply frequency also increases.

Bibliography



1. Salah, D. G. Dorrell, and Y. Guo, “A review of the monitoring and damping unbalanced magnetic pull in induction machines due to rotor eccentricity,” in *IEEE Transactions on Industry Applications*, May 2019, vol. 55, no. 3, pp. 2569–2580. doi: 10.1109/TIA.2019.2892359.
2. J. Faiz, B. M. Ebrahimi, and M. B. B. Sharifian, “Different faults and their diagnosis techniques in three-phase squirrel-cage induction motors-a review,” *Electromagnetics*, vol. 26, no. 7, pp. 543–569, Oct. 2006, doi: 10.1080/02726340600873003.
3. A. Burakov and A. Arkkio, “Comparison of the unbalanced magnetic pull mitigation by the parallel paths in the stator and rotor windings,” *IEEE Transactions on Magnetics*, vol. 43, no. 12, pp. 4083–4088, Dec. 2007, doi: 10.1109/TMAG.2007.906885
4. J. Martinez, A. Belahcen, and A. Arkkio, “A 2D FEM model for transient and fault analysis of induction machines,” in *Przeglad Elektrotechniczny*, 2012, pp. 157-160.
5. R. Deore, B. Brahma, Shahrukh, and K. Kalita, “The Passive Vibration Control in Bridge Configured Winding Cage Rotor Induction Motor: An Experimental Analysis”, *International Conference on Rotordynamics*, <https://doi.org/10.1007/978-3-031-40455-9>.
6. D. Guo, F. Chu, and D. Chen, “The unbalanced magnetic pull and its effects on vibration in a three-phase generator with eccentric rotor,” *Journal of Sound & Vibrations*, vol. 254, no. 2, pp. 297–312, Jul. 2003, doi: 10.1006/jsvi.2001.4088.

Thank You